18F-fluoride positron emission tomography for identification of ruptured and high-risk coronary atherosclerotic plaques: a prospective clinical trial

^{18}F-fluoride positron emission tomography for identification of ruptured and high-risk coronary atherosclerotic plaques: a prospective clinical trial

Nikhil V Joshi, Alex T Vesey, Michelle C Williams, Anoop S V Shah, Patrick A Calvert, Felicity H M Craighead, Su Ern Yeoh, William Wallace, Donald Salter, Alison M Fletcher, Edwin J R van Beek, Andrew D Flapan, Neal G Uren, Miles W H Behan, Nicholas L M Cruden, Nicholas L Mills, Keith A A Fox, James H F Rudd, Marc R Dweck, David E Newby**

Summary

Background **The use of non-invasive imaging to identify ruptured or high-risk coronary atherosclerotic plaques would represent a major clinical advance for prevention and treatment of coronary artery disease. We used combined PET and CT to identify ruptured and high-risk atherosclerotic plaques using the radioactive tracers ^{18}F-sodium fluoride (^{18}F-NaF) and ^{18}F-fluorodeoxyglucose (^{18}F-FDG).**

Methods **In this prospective clinical trial, patients with myocardial infarction (n=40) and stable angina (n=40) underwent ^{18}F-NaF and ^{18}F-FDG PET-CT, and invasive coronary angiography. ^{18}F-NaF uptake was compared with histology in carotid endarterectomy specimens from patients with symptomatic carotid disease, and with intravascular ultrasound in patients with stable angina. The primary endpoint was the comparison of ^{18}F-fluoride tissue-to-background ratios of culprit and non-culprit coronary plaques of patients with acute myocardial infarction.**

Findings **In 37 (93%) patients with myocardial infarction, the highest coronary ^{18}F-NaF uptake was seen in the culprit plaque (median maximum tissue-to-background ratio: culprit 1·66 [IQR 1·40–2·25] *vs* highest non-culprit 1·24 [1·06–1·38], p<0·0001). By contrast, coronary ^{18}F-FDG uptake was commonly obscured by myocardial uptake and where discernible, there were no differences between culprit and non-culprit plaques (1·71 [1·40–2·13] *vs* 1·58 [1·28–2·01], p=0·34). Marked ^{18}F-NaF uptake occurred at the site of all carotid plaque ruptures and was associated with histological evidence of active calcification, macrophage infiltration, apoptosis, and necrosis. 18 (45%) patients with stable angina had plaques with focal ^{18}F-NaF uptake (maximum tissue-to-background ratio 1·90 [IQR 1·61–2·17]) that were associated with more high-risk features on intravascular ultrasound than those without uptake: positive remodelling (remodelling index 1·12 [1·09–1·19] *vs* 1·01 [0·94–1·06]; p=0·0004), microcalcification (73% *vs* 21%, p=0·002), and necrotic core (25% [21–29] *vs* 18% [14–22], p=0·001).**

Interpretation **^{18}F-NaF PET-CT is the first non-invasive imaging method to identify and localise ruptured and high-risk coronary plaque. Future studies are needed to establish whether this method can improve the management and treatment of patients with coronary artery disease.**

Funding **Chief Scientist Office Scotland and British Heart Foundation.**

Published **Online** November 11, 2013 http://dx.doi.org/10.1016/S0140-6736(13)61754-7

See **Online/Comment** http://dx.doi.org/10.1016/S0140-6736(13)61911-X

*These authors contributed equally

Centre for Cardiovascular Science, Clinical Research Imaging Centre, and Division of Pathology, University of Edinburgh, Edinburgh, UK (N V Joshi MD, A T Vesey MD, M C Williams MD, A S V Shah MD, F H M Craighead BSc, S E Yeoh, W Wallace MD, D Salter MD, A M Fletcher PhD, E J R van Beek PhD, N L Mills PhD, Prof K A A Fox MD, M R Dweck PhD, Prof D E Newby DSc)**; Edinburgh Heart Centre, Royal Infirmary of Edinburgh, Edinburgh, UK** (A D Flapan MD, N G Uren MD, M W H Behan MD, N L M Cruden PhD)**; and Division of Cardiovascular Medicine, University of Cambridge, Cambridge, UK** (P A Calvert PhD, J H F Rudd PhD)

Correspondence to:
Dr Nikhil Vilas Joshi, SU 305, Chancellors Building, University/BHF Centre for Cardiovascular Science, Little France Crescent, Edinburgh, UK
nikhil.joshi@ed.ac.uk

Introduction

Coronary atherosclerotic plaque rupture is the principal precipitant of acute myocardial infarction and an important cause of sudden cardiac death. Rupture is challenging to predict because most plaques are non-obstructive and are not identified by stress testing or coronary angiography.[1,2] Atherosclerotic lesions at risk of rupture have certain histopathological characteristics that include positive remodelling, microcalcification, and a large necrotic core.[1–3] The development of modern molecular imaging techniques targeted at these features could lead to the identification of such high-risk plaques in vivo and guide the development of novel treatment strategies.[4–7]

Combined PET and CT is a non-invasive imaging technique that brings functional molecular imaging together with precise anatomical information. We have recently reported preliminary PET-CT data using the tracer ^{18}F-sodium fluoride (^{18}F-NaF) as a marker of valvular and vascular calcification activity in patients with aortic stenosis.[7–9] Other studies have shown the usefulness of ^{18}F-flurodeoxyglucose (^{18}F-FDG) as a surrogate of vascular inflammation and macrophage burden.[6,10–13] We therefore investigated whether, compared with the current non-invasive gold standard of ^{18}F-FDG, ^{18}F-NaF uptake could identify ruptured and high-risk atherosclerotic plaques in patients with symptomatic coronary and carotid artery disease.

Methods

Patients

Patients were recruited from the Royal Infirmary of Edinburgh between February, 2012, and January, 2013, in three cohorts: 40 patients with acute ST-segment or non-ST-segment elevation myocardial infarction,[14] 40 patients with stable angina pectoris undergoing elective invasive coronary angiography, and 12 patients (nine evaluable)

undergoing carotid endartectomy for symptomatic carotid artery disease.[15]

Exclusion criteria were age younger than 50 years, insulin-dependent diabetes mellitus, women of childbearing age not receiving contraception, severe renal failure (serum creatinine >250 μmol/L), known contrast allergy, and inability to provide informed consent. Only patients older than 50 years were recruited in the study to reduce any long-term risks associated with radiation exposure. Uncontrolled diabetes and high blood glucose concentrations (>11 mmol/L) interfere with the quality of ^{18}F-FDG PET imaging because of the competition between glucose and ^{18}F-FDG for cellular entry. The convention is therefore to exclude such patients from vascular ^{18}F-FDG PET studies.[7,10,12,13]

All patients underwent a comprehensive baseline clinical assessment including evaluation of their cardiovascular risk factor profile. Plasma troponin I concentrations were measured in patients with stable angina using the ARCHITECT STAT high-sensitivity troponin I assay (Abbott Laboratories, Abbott Park, IL, USA; lower limit of detection 1·2 ng/L; 99th percentile diagnostic threshold 26 ng/L). Studies were done with the approval of the local research ethics committee, in accordance with the Declaration of Helsinki, and with the written informed consent of each participant.

Procedures

Patients with myocardial infarction and stable angina underwent ^{18}F-NaF and ^{18}F-FDG PET-CT, CT coronary angiography, and CT calcium scoring (appendix).[7] To minimise myocardial uptake, patients were instructed to adhere to a low-carbohydrate, high-protein, and high-fat diet for at least 24 h before undergoing ^{18}F-FDG PET-CT.

See Online for appendix

Electrocardiograph-gated PET images were reconstructed in diastole (50–75% of the R-R interval, Ultra-HD) using the Siemens Ultra-HD algorithm, fused with the CT coronary angiogram, and analysed by experienced observers blinded to the clinical diagnosis (NJ, MD, FC) using an OsiriX workstation (OsiriX version 5·5·1 64-bit; OsiriX Imaging Software, Geneva, Switzerland). Two-dimensional regions of interest were drawn around all major (diameter >2 mm) epicardial vessels on 3 mm axial slices just beyond the discernible adventitial border. The maximum standard uptake value (the decay corrected tissue concentration of the tracer divided by the injected dose per bodyweight) was measured and corrected for blood pool activity in the superior vena cava to provide tissue-to-background ratio (TBRs) measurements. Using this method, we have previously shown excellent reproducibility for ^{18}F-NaF TBR measurements in the coronary arteries with an intraclass correlation coefficient of 0·99.[7]

We used a previously established 95% lower reference limit to categorise coronary plaques into ^{18}F-NaF positive lesions (focal uptake with a TBR more than 25% higher than a proximal reference lesion) and negative plaques if these criteria were not achieved. This limit was based on our previous study, where plaques with high ^{18}F-NaF uptake had maximum TBRs that were 44% (95% CI 26–62) higher than a proximal quiescent reference lesion.[7] In patients with acute myocardial infarction, ^{18}F-NaF uptake in the culprit plaque was compared with the highest value in any of the non-culprit vessels.

Quantification of ^{18}F-FDG uptake was performed as for ^{18}F-NaF uptake but restricted to the proximal and mid-portions of the coronary arteries, and to regions where myocardial uptake and spillover could be confidently excluded.[7] Again, ^{18}F-FDG positive plaques were defined using the 25% threshold as described for ^{18}F-NaF. Effective myocardial suppression of ^{18}F-FDG was predefined as a standard uptake value of 5·0 or less in the basal ventricular septum (appendix) as per published data.[12]

In patients with stable angina, PET-CT imaging was prospectively used to direct greyscale and radiofrequency intravascular ultrasound (20 MHz Eagle Eye Platinum Catheters [Volcano Corp, San Diago, CA, USA], motorised pull-back 0·5 mm/s) to the ^{18}F-NaF positive and negative plaques. The interventional cardiologist acquiring the intravascular ultrasound data was blinded to the PET-CT status of the plaque.

Intravascular ultrasound analysis was done as described previously[16] using dedicated VIAS software (Volcano Image Analysis Software version 3.0) by operators blinded to the PET data. Regions of interest were drawn around the external elastic membrane and luminal borders, and plaque area and composition (dense calcium, necrotic core, fibro-fatty tissue, and fibrous tissue) calculated.[16–18] The presence of microcalcification (spotty calcification in the absence of acoustic shadowing on three or more consecutive frames) and the maximum frame necrotic core (the highest percentage of necrotic core on a single frame) were recorded.[19] The remodelling index was defined as the ratio between the external elastic membrane cross-sectional area of the lesion and a proximal reference region in the same vessel.[20] Plaques were classified as thin-cap fibroatheroma, thick-cap fibroatheroma, pathological intimal thickening, or fibrocalcific plaque as defined previously.[18,21]

CT analysis was done on a dedicated cardiovascular workstation (Vital Images, Minnetonka, MN, USA). Vessel-specific and total Agatston calcium scores were calculated as described previously.[7] An independent experienced and blinded observer (MW) determined the stenosis severity, plaque composition (calcified, non-calcified, mixed plaque), and presence of high-risk CT features (positive remodelling, microcalcification, necrotic core) according to standard definitions in plaques with and without increased ^{18}F-NaF activity.[22]

Intact atherosclerotic plaques were retrieved at the time of carotid endarterectomy and scanned using ex-vivo PET-CT to allow precise anatomical colocalisation of ^{18}F-NaF activity with pathological evidence of plaque rupture. Plaques were divided into ^{18}F-NaF positive and negative areas, and histological sections were assessed

using Movat's pentachrome and immunohistochemistry to investigate calcification activity (tissue non-specific alkaline phosphatase and osteocalcin), macrophage infiltration (CD68), and cell death (apoptosis, cleaved caspase 3; presence of necrotic core; appendix).

Statistical analysis

The primary endpoint of the study was the comparison of ^{18}F-fluoride tissue-to-background ratios of culprit and non-culprit coronary plaques of patients with acute myocardial infarction. The main secondary endpoints were comparative imaging and histological characterisation of ^{18}F-fluoride positive and negative atherosclerotic plaques in patients with coronary and carotid artery disease. Based on our previous data,[7] we required 36 patients with myocardial infarction to detect a difference of 0·23 in the tissue-to-background ratio between culprit and non-culprit plaques at 90% power and two-sided p<0·05. We recruited 40 patients to account for incomplete data and recruited a similar sized (n=40) comparator group of patients with stable angina.

Continuous data were tested for normality with the D'Agostino-Pearson omnibus test. Continuous parametric variables were expressed as mean (SD) and

	Myocardial infarction			Stable angina All (n=40)
	All (n=40)	STEMI (n=26)	NSTEMI (n=14)	
Age in years, mean (SD)	62 (8)	63 (9)	60 (8)	67 (8)
Men, n (%)	37 (93%)	24 (92%)	13 (93%)	36 (90%)
Body-mass index (kg/m^2), mean (SD)	28 (5)	27 (5)	30 (4)	30 (5)
Antecedent angina (active), n (%)	9 (23%)	5 (19%)	4 (29%)	40 (100%)
Heart rate (per min), mean (SD)*	56 (7)	56 (7)	56 (7)	59 (9)
Systolic blood pressure (mm Hg), mean (SD)	132 (21)	131 (20)	121 (21)	134 (14)
Diastolic blood pressure (mm Hg), mean (SD)	76 (9)	76 (9)	76 (8)	77 (10)
Cardiovascular history, n (%)				
Previous MI	5 (13%)	1 (4%)	4 (29%)	15 (38%)
Previous CVA/TIA	2 (5%)	1 (4%)	1 (7%)	4 (10%)
Previous PCI	5 (13%)	2 (8%)	3 (21%)	19 (48%)
Previous CABG	2 (5%)	2 (8%)	0	11 (28%)
Risk factors, n (%)				
Smoking habit (ex or current)	25 (63%)	19 (73%)	6 (43%)	24 (60%)
Non-insulin dependent diabetes	8 (20%)	7 (27%)	1 (7%)	13 (33%)
Hypertension	17 (43%)	11 (42%)	6 (43%)	36 (90%)
Hypercholesterolaemia	19 (48%)	11 (42%)	8 (57%)	39 (98%)
Medications, n (%)†				
Aspirin	40 (100%)	26 (100%)	14 (100%)	33 (83%)
Clopidogrel	39 (98%)	25 (96%)	14 (100%)	5 (13%)
Statin	39 (98%)	26 (100%)	13 (93%)	36 (90%)
β blocker	32 (80%)	20 (77%)	12 (86%)	28 (70%)
ACEI/ARB	35 (88%)	25 (96%)	10 (71%)	20 (50%)
Calcium channel blockers	2 (5%)	2 (8%)	0	16 (40%)
Other anti-hypertensive	3 (8%)	1 (4%)	2 (14%)	6 (15%)
Oral nitrates	1 (3%)	0	1 (7%)	15 (38%)
Serum biochemistry, mean (SD)				
Cholesterol (mmol/L)	4·7 (1·2)	4·7 (1·3)	4·8 (1·1)	3·9 (0·8)
HDL cholesterol (mmol/L)	1·1 (0·3)	1·1 (0·3)	1·0 (0·3)	1·1 (0·3)
LDL cholesterol (mmol/L)	2·9 (1·1)	2·8 (1·1)	3·1 (1·0)	2·1 (0·7)
Triglycerides (mmol/L)	1·6 (0·8)	1·7 (0·7)	1·5 (0·7)	1·6 (0·7)
Creatinine (μmol/L)	84 (27)	86 (29)	82 (24)	85 (23)
Coronary artery calcium score (Agatston units), median (IQR)	159 (42–456)	176 (45–474)	122 (26–442)	599 (60–1302)
Peak troponin concentration (ng/L), median (IQR)	32 300 (10 200–50 000)	11 200 (3300–50 000)	3800 (1000–9200)	

NSTEMI=non-ST elevation myocardial infarction. MI=myocardial infarction. CVA=cerebrovascular accident. TIA=transient ischaemic attack. PCI=percutaneous coronary intervention. ACEI=angiotensin converting enzyme inhibitor. ARB=angiotensin receptor blocker. CABG=coronary artery bypass graft. HDL=high-density lipoprotein. LDL=low-density lipoprotein. STEMI=ST-elevation myocardial infarction. *Heart rate at the time of CT coronary angiography. †Medications at the time of scan.

Table 1: **Baseline characteristics of patients with coronary artery disease**

compared using Student's *t* tests. Non-parametric data were presented as median (IQR) and compared using Mann-Whitney *U* test or Wilcoxon signed-rank test as appropriate. Fisher's exact test or chi-squared test was used for analysis of categorical variables. Statistical analysis was done with Graph Pad Prism version 5 (GraphPad Software, La Jolla, CA, USA). A two-sided p<0·05 was taken as statistically significant.

The study was registered with ClinicalTrials.gov number NCT01749254.

Role of the funding source

The funding source had no role in the study design (except through its external peer review process), data collection, data analysis, data interpretation, or writing of the report. All authors had access to the primary data and have final responsibility to submit for publication.

Results

Patients were predominantly middle-aged men and had multiple cardiovascular risk factors (table 1). They underwent both ^{18}F-NaF (60 [SD 9] min after 123 [SD 5] MBq) and ^{18}F-FDG (90 [7] min after 192 [11] MBq) PET-CT scanning within a median of 6 (IQR 3–9) days. The median duration between PET-CT scanning and coronary angiography was 7 (IQR 1–12) days. The total effective radiation dose from study participation was 13·7 (SD 3·0) mSv (conversion factor of 0·014 mSv/mGy.cm): ^{18}F-NaF (3·8 [SD 0·3] mSv) and ^{18}F-FDG (4·9 [0·5] mSv) PET-CT, CT coronary angiogram (3·7 [2·1] mSv), and calcium score (1·3 [0·5] mSv).

The culprit vessel was the left anterior descending artery in 17 (42%) patients, the left circumflex artery in seven (18%), and the right coronary artery in 16 (40%). Patients underwent ^{18}F-NaF scans 6 [IQR 3–10] days after hospitalisation for myocardial infarction (symptoms to ^{18}F-NaF scan, 8 [3–10] days). ^{18}F-NaF activity in the culprit plaque was 34% higher than the maximum activity recorded anywhere else in the coronary vasculature (maximum TBR 1·66 [1·40–2·25] *vs* 1·24 [1·06–1·38], p<0·0001; figures 1 and 2). In 37 of the 40 patients (93%), increased ^{18}F-NaF uptake was seen in the culprit plaque (figure 1; appendix). In the three patients without uptake, two were younger smokers (aged 50 and 52 years) and, in the third, the culprit lesion was adjudicated as the right coronary artery although focal increased activity was seen in the left circumflex artery. In five patients, increased ^{18}F-NaF activity was seen at multiple sites within the coronary circulation.

Predefined myocardial suppression of ^{18}F-FDG uptake was achieved in 28 (70%) patients (median myocardial standard uptake value 3·92 [IQR 2·71–5·55]). However, coronary ^{18}F-FDG uptake could not be distinguished from patchy myocardial uptake in 22 patients affecting 52% of vessel territories. Increased uptake of ^{18}F-FDG was observed in the culprit vessels of six (33%) of the remaining 18 patients. Overall, no significant differences could be shown between the maximum TBRs in the culprit plaques and those recorded elsewhere in the coronary vasculature (1·71 [IQR 1·40–2·13] *vs* 1·58 [1·28–2·01], p=0·34: figure 2) with a mean difference of 0·09 (95% CI –0·07 to 0·24).

The median duration between clinical symptoms and carotid endarterectomy was 17 [IQR 10–27] days (appendix). Carotid endarterectomy specimens (figure 3; appendix) were obtained for 12 patients, although three specimens could not be excised intact and were discarded. Ex-vivo ^{18}F-NaF PET-CT was undertaken in nine specimens and uptake was localised to the site of macroscopic plaque rupture in all patients (figure 3). Compared with sections of tissue without uptake (n=15), those with increased ^{18}F-NaF uptake (n=24) had increased calcification activity (tissue non-specific alkaline phosphatase 4·07% [SD 3·42] *vs* 0·76% [0·51], p<0·0001; osteocalcin 1·88% [IQR 0·58–4·10] *vs* 0·25% [0·11–0·58], p<0·0001), macrophage infiltration (CD68, 350 [IQR 172–840] *vs* 145 [24–362] cells/mm², p=0·013), and cell death (apoptosis, cleaved-caspase-3, 1·23% [0·69–1·91] *vs* 0·09% [0·04–1·38], p=0·005; necrotic core, 22/24 *vs* 4/15; p<0·0001; appendix).

Patients with stable angina were older (67 [SD 8] *vs* 62 [8] years, p=0·006) and had more severe coronary artery disease (coronary artery calcium score 599 [IQR 60–1302] *vs* 159 [42–456] Agatston units, p=0·006) than those with myocardial infarction (table 1). Focal ^{18}F-NaF uptake was noted in 18 patients (45%), which did not seem to be related to percutaneous coronary intervention and stent

Figure 1: **Focal ^{18}F-fluoride and ^{18}F-fluorodeoxyglucose uptake in patients with myocardial infarction and stable angina**

Patient with acute ST-segment elevation myocardial infarction with (A) proximal occlusion (red arrow) of the left anterior descending artery on invasive coronary angiography and (B) intense focal ^{18}F-fluoride (^{18}F-NaF, tissue-to-background ratios, culprit 2·27 versus reference segment 1·09 [108% increase]) uptake (yellow-red) at the site of the culprit plaque (red arrow) on the combined positron emission and computed tomogram (PET-CT). Corresponding ^{18}F-fluorodeoxyglucose PET-CT image (C) showing no uptake at the site of the culprit plaque (^{18}F-FDG, tissue-to-background ratios, 1·63 versus reference segment 1·91 [15% decrease]). Note the significant myocardial uptake overlapping with the coronary artery (yellow arrow) and uptake within the oesophagus (blue arrow). Patient with anterior non-ST-segment elevation myocardial infarction with (D) culprit (red arrow; left anterior descending artery) and bystander non-culprit (white arrow; circumflex artery) lesions on invasive coronary angiography that were both stented during the index admission. Only the culprit lesion had increased ^{18}F-NaF uptake (^{18}F-NaF, tissue-to-background ratios, culprit 2·03 versus reference segment 1·08 [88% increase]) on PET-CT (E) after percutaneous coronary intervention. Corresponding ^{18}F-fluorodeoxyglucose PET-CT showing no uptake either at the culprit (^{18}F-FDG, tissue-to-background ratios, culprit 1·62 versus reference segment 1·49 [9% increase]) or the bystander stented lesion. Note intense uptake within the ascending aorta. In a patient with stable angina with previous coronary artery bypass grafting, invasive coronary angiography (G) showed non-obstructive disease in the right coronary artery. Corresponding PET-CT scan (H) showed a region of increased ^{18}F-NaF activity (positive lesion, red line) in the mid-right coronary artery (tissue-to-background ratio, 3·13) and a region without increased uptake in the proximal vessel (negative lesion, yellow line). Radiofrequency intravascular ultrasound shows that the ^{18}F-NaF negative plaque (I) is principally composed of fibrous and fibrofatty tissue (green) with confluent calcium (white with acoustic shadow) but little evidence of necrosis. On the contrary, the ^{18}F-NaF positive plaque (J) shows high-risk features such as a large necrotic core (red) and microcalcification (white).

deployment (appendix). The maximum TBR for ^{18}F-NaF positive plaques was 1·90 [IQR 1·61–2·17] and for ^{18}F-NaF negative plaques was 1·02 [0·82–1·17]. ^{18}F-NaF positive plaques were predominantly (72% of patients) non-obstructive (<70% luminal stenosis) on coronary angiography and showed multiple high-risk features on radiofrequency intravascular ultrasound (positive remodelling [remodelling index 1·12 [IQR 1·09–1·19] *vs*

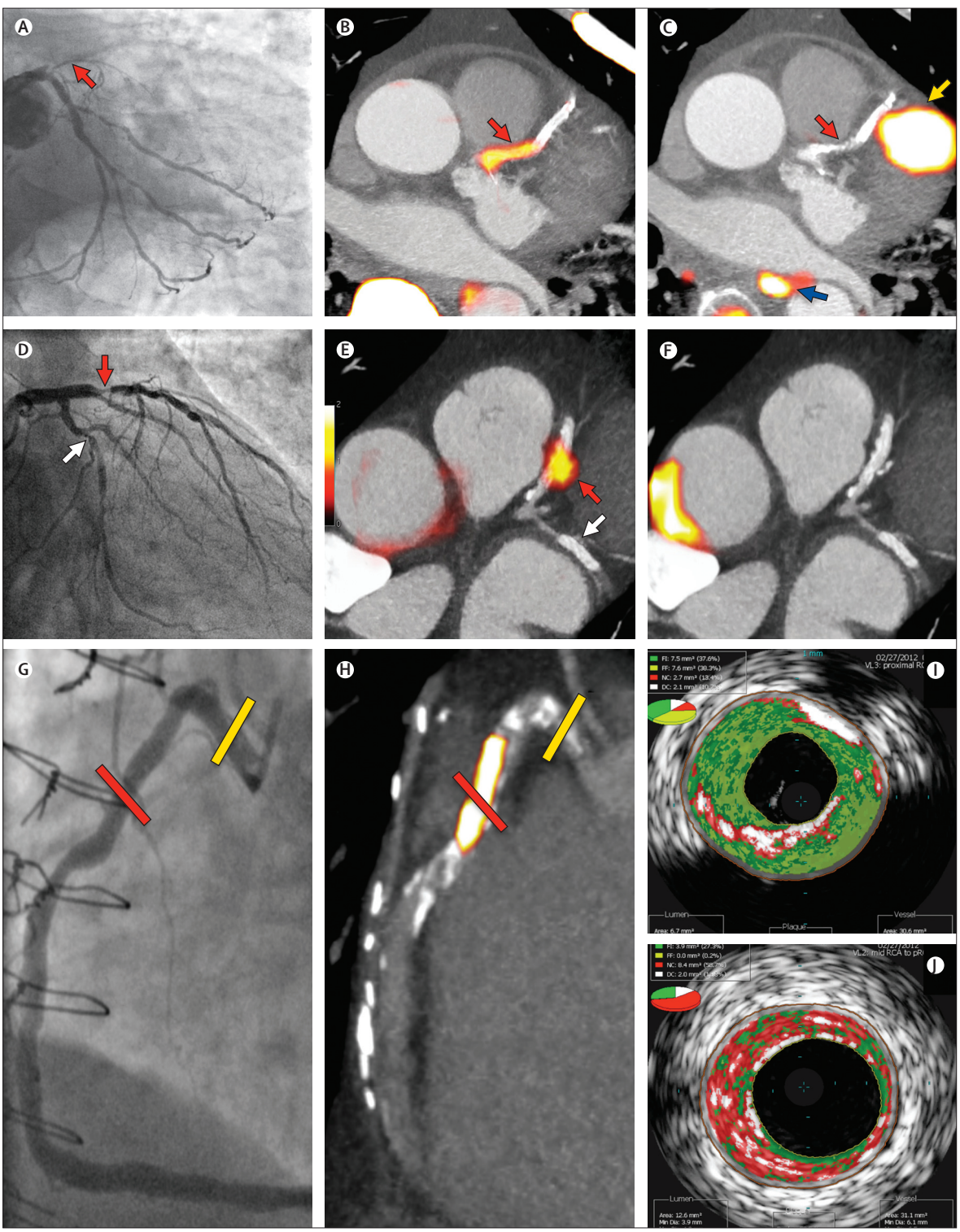

1·01 [0·94–1·06]; p<0·001, microcalcification (73 *vs* 21%, p=0·002) and necrotic core (24·6% [20·5–28·8] *vs* 18·0% [14·0–22·4]), p=0·001), with similar observations for CT (figure 1, table 2; appendix). Multivessel uptake was commonly seen: two-vessel uptake in six (15%) and three-vessel uptake in five (13%) patients. Patients with ^{18}F-NaF positive lesions had higher concentrations of plasma troponin at baseline (3·35 [IQR 2·35–10·20] *vs* 2·45 [1·85–4·02] ng/L; p=0·047), with one individual having a concentration (35 ng/L) above the 99th percentile diagnostic threshold.

Although predefined myocardial suppression of ^{18}F-FDG uptake was achieved in 34 (85%) patients (median myocardial standard uptake value 2·60 [IQR 1·83–3·83]), coronary ^{18}F-FDG uptake could not be confidently interpreted in 45% of vessel territories. Increased focal ^{18}F-FDG uptake was noted in just four patients: three at the site of recent coronary stenting and one at the ostium of a saphenous vein graft.

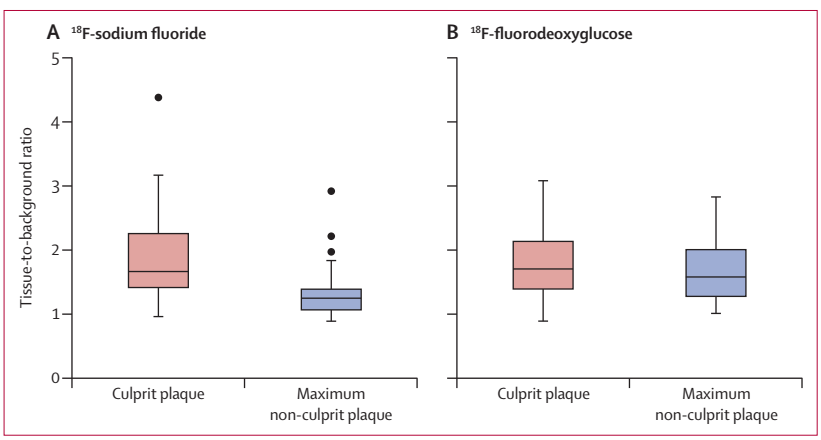

Figure 2: **^{18}F-fluoride and ^{18}F-fluorodeoxyglucose uptake in patients with myocardial infarction**
^{18}F-fluoride activity (maximum tissue-to-background ratio) was increased in the culprit plaque (red) compared with the maximum uptake in any of the non-culprit plaques (blue). By contrast, there was no difference in the activity of ^{18}F-fluorodeoxyglucose between these regions.

Discussion

We have shown that intense ^{18}F-NaF uptake localises to recent plaque rupture in patients with acute myocardial infarction and in those with symptomatic carotid disease. Moreover, in patients with stable coronary artery disease, ^{18}F-NaF uptake seems to identify coronary plaques with high-risk features on intravascular ultrasound. This technique holds major promise as a means of identifying high-risk and ruptured plaque, and potentially informing the future management and treatment of patients with stable and unstable coronary artery disease.

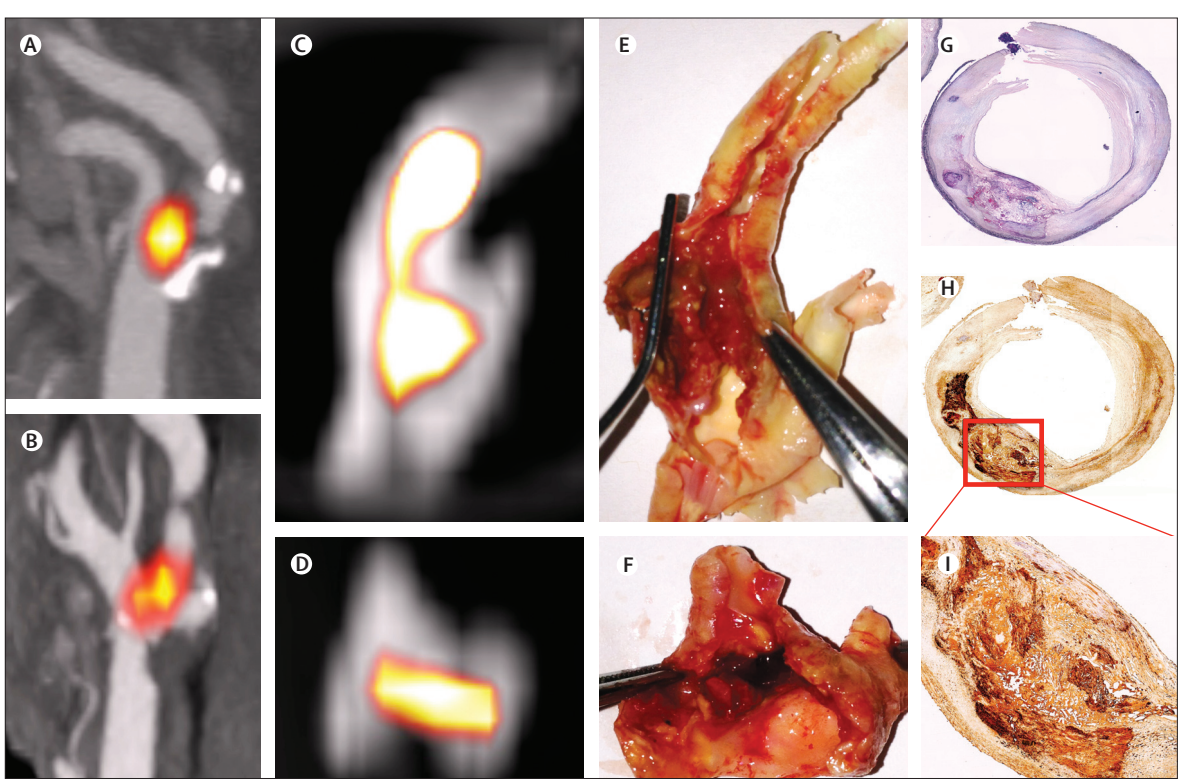

Figure 3: **Carotid ^{18}F-fluoride uptake and carotid plaque rupture**
In-vivo (A and B) and ex-vivo (C and D) positron emission and computed tomograms showing colocalisation of ^{18}F-fluoride (^{18}F-NaF) uptake (yellow-orange) to the site of plaque rupture with adherent thrombus on excised carotid endarterectomy tissue (E and F). Histology of the ^{18}F-NaF-positive region shows a large necrotic core (Movat's pentachrome, magnification 4×, G), within which increased staining for tissue non-specific alkaline phosphatase can be seen as a marker of calcification activity on immunohistochemistry (magnification 4×, H; magnification 10×, I).

Over 90% of our patients with myocardial infarction had increased ^{18}F-NaF uptake at the site of their culprit ruptured plaque, with TBR values that were a third higher than the maximum activity anywhere else in the coronary vasculature. These findings were not unique to the coronary circulation since we also noted increased focal ^{18}F-NaF uptake at the site of plaque rupture in all excised carotid endarterectomy specimens from patients with symptomatic carotid disease. However, we do acknowledge that this was not a universal finding. Of the three patients with myocardial infarction who had no uptake, two were younger smokers with only mild underlying irregularities on coronary angiography, implicating plaque erosion and thrombosis as the mechanism of their infarction rather than plaque rupture.[23] The third patient sustained an inferolateral non-ST segment elevation myocardial infarction and had a lesion stented in the right coronary artery. Increased ^{18}F-NaF activity was seen in the co-dominant circumflex artery that could have equally explained the clinical presentation, raising the intriguing possibility that ^{18}F-NaF might have a clinical role for patients in whom the culprit lesion is not readily apparent.

Focal regions of increased ^{18}F-NaF activity were seen in almost a half of our patients with stable coronary artery disease. To understand the mechanism of uptake in these patients, we sought to compare plaque characteristics of lesions with and without increased ^{18}F-NaF uptake. Because histology of the coronary arteries in this population is not feasible, we undertook greyscale and radiofrequency intravascular ultrasound, a widely used and validated process that provides detailed characterisation of plaque composition.[21] This method showed that lesions with increased ^{18}F-NaF uptake were associated with greater positive remodelling, more microcalcification, and a larger necrotic core. These findings were corroborated by, and consistent with, the findings of plaque analysis done with CT coronary angiography. Plasma troponin concentrations measured by a novel high-sensitivity assay were also higher in those patients with ^{18}F-NaF positive plaques than in patients with ^{18}F-NaF negative plaques, perhaps implicating subclinical plaque rupture with embolisation and microinfarction.

Why does ^{18}F-NaF bind to ruptured or high-risk plaque? Similar to the caseating granulomata of tuberculosis, atherosclerotic vascular calcification is a controlled cellular response to an intense, necrotic, and chronic inflammatory stimulus. Indeed, direct links between inflammatory cells and osteoblastic metaplasia in the vasculature are well described.[24,25] Hydroxyapatite is the central structural component of vascular calcification and is laid down during the earliest and most active stages of mineralisation:[24] hydroxyapatite nanocrystals nucleate, propagate, and mineralise the extracellular matrix. Fluoride ions are incorporated into the hydroxyapatite by ion exchange with hydroxyl groups at the crystal surface. This process is dependent on the crystal surface area that will be greatest in the earliest and most active nanocrystalline stages of mineralisation associated with plaque inflammation and necrosis. We believe that these processes are responsible for the observed ^{18}F-NaF uptake and is consistent with our data showing ^{18}F-NaF uptake in regions of necrosis, macrophage infiltration, apoptosis, microcalcification, and alkaline phosphatase and osteocalcin staining. Moreover, mathematical modelling indicates that microcalcification at the surface of thin-capped atheroma (figure 1) can intensify and double incident stresses.[26] Microcalcification is therefore not only a marker of acute plaque rupture but is implicated in its precipitation.

Coronary arterial calcification is considered pathognomonic of atherosclerosis and is a powerful independent risk predictor for cardiovascular events that can be further refined by the rapidity of its progression.[27,28] Why then not rely on CT coronary calcium scoring alone as a biomarker? Microcalcification cannot be detected on CT and confluent coronary macrocalcification develops slowly, taking many months or years to become apparent on CT, and can become dormant once inflammation in

	^{18}F-fluoride positive plaques (n=15)	^{18}F-fluoride negative plaques (n=24)	p
Lumen			
Area (mm²)	9·0 (5·7–13·5)	6·7 (4·7–9·7)	0·078
Minimal diameter (mm)	2·6 (1·7–3·1)	1·9 (1·7–2·6)	0·165
Maximum diameter (mm)	4·9 (4·1–5·3)	3·6 (3·1–4·6)	0·006
Vessel			
Area (mm²)	24·1 (17·2–27·1)	14·5 (11·9–18·1)	0·002
Minimal diameter (mm)	4·4 (3·4–5·2)	3·6 (3·0–4·1)	0·057
Maximum diameter (mm)	6·5 (6·0–7·1)	5·2 (4·7–5·9)	0·0001
Plaque			
Length (mm)	14·2 (6·2–23·5)	15·2 (6·7–25·0)	0·941
Volume (mm³)	152·9 (99·6–289·7)	91·0 (45·8–158·2)	0·032
Burden (%)*	55·6 (48·6–64·4)	54·2 (46·3–57·3)	0·174
Remodelling index	1·12 (1·09–1·19)	1·01 (0·94–1·06)	0·0004
Plaque composition			
Fibrous tissue (%)	51·0 (46·3–56·6)	58·1 (51·6–65·5)	0·015
Fibro-fatty (%)	10·9 (6·0–13·8)	12·6 (9·3–17·8)	0·092
Necrotic core (%)	24·6 (20·5–28·8)	18·0 (14·0–22·4)	0·001
Maximum frame necrotic core (%)†	35·5 (34·2–40·5)	29·2 (23·9–42·1)	0·009
Dense calcium (%)	12·6 (9·1–18·1)	10·2 (4·0–14·9)	0·092
Microcalcification, n (%)	11 (73%)	5 (21%)	0·002
Plaque classification, n (%)			
Thin-cap fibroatheroma	7 (47%)	4 (16%)	0·068
Thick-cap fibroatheroma	5 (33%)	9 (38%)	1·0
Pathological intimal thickening	0	7 (29%)	0·003
Fibrocalcific plaque	3 (20%)	4 (16%)	1·0

Data are median (IQR) unless otherwise stated. *Plaque burden calculation = (average vessel area – average lumen area) /average vessel area. †Maximum necrotic core in any single frame in the plaque.

Table 2: **Greyscale and radiofrequency intravascular ultrasound characteristics in ^{18}F-fluoride positive and negative plaques of patients with stable angina**

Panel: Research in context

Systematic review

We searched PubMed using variations of the keywords "high-risk plaques", "vulnerable plaques", "ruptured plaques", "^{18}F-fluorodeoxyglucose positron emission tomography", "^{18}F-fluoride positron emission tomography", and "coronary arteries". The search was restricted to human studies. We assessed the quality of the evidence specifically related to cardiovascular disease by reviewing the patient population studied and the methodology for the positron emission and CT imaging.

Non-invasive imaging of carotid plaque inflammation using ^{18}F-fluorodeoxyglucose positron emission tomography was reported by Rudd and colleagues in 2002.[11] Since then, this tracer has been validated and widely used as a surrogate of large vessel inflammation.[8,10] Increased ^{18}F-fluorodeoxyglucose in the coronary arteries has been described in patients with coexisting malignancy.[12,33,34] Since then, three prospective studies have examined the feasibility and reproducibility of assessing uptake of this tracer in the coronary vasculature.[6,7,13] Only two small studies (n=10–20)[6,13] have suggested that ^{18}F-fluorodeoxyglucose might identify some inflamed plaques in patients with recent myocardial infarction, although the largest study showed that in 50% of patients with acute myocardial infarction, there was no uptake of ^{18}F-fluorodeoxyglucose in the culprit plaque.[13]

Four retrospective studies in patients with cancer have recently reported cardiovascular uptake of ^{18}F-fluoride.[29,31,32,35] The aortic uptake of ^{18}F-NaF was first reported by Derlin and colleagues[29] and cardiac ^{18}F-fluoride uptake by Beheshti and colleagues.[31] We reported the coronary uptake of ^{18}F-NaF in a prospective clinical trial involving patients with aortic stenosis,[7,8] and these results were subsequently corroborated by Li and colleagues in their retrospective study of patients with cancer.[30] No study has prospectively assessed this tracer in patients with stable or unstable coronary artery disease or validated its activity against histology or invasive intracoronary imaging, such as intravascular ultrasound. There are no previous reports of ^{18}F-fluoride uptake in relation to plaque vulnerability or rupture.

Interpretation

There are currently no non-invasive imaging techniques that can identify high-risk and ruptured coronary atherosclerotic plaques in vivo in patients with coronary heart disease. For the first time, we have shown that ^{18}F-fluoride positron emission tomography can identify culprit and ruptured plaques in patients with myocardial infarction and symptomatic carotid disease. Moreover, histological characterisation demonstrates that ^{18}F-fluoride activity localises to regions of plaque rupture with evidence of increased inflammation, calcification activity, necrosis, and cell death. In patients with stable angina, ^{18}F-fluoride is associated with coronary plaques that have high-risk features on intravascular ultrasound, including positive remodelling, microcalcification, and necrosis. Given its ability to identify high-risk or ruptured coronary atherosclerotic plaque, this non-invasive imaging technique has the potential to change how we identify, manage, and treat patients with stable and unstable coronary artery disease. Further work is now needed to establish whether ^{18}F-fluoride positron emission tomography will provide a means of improving risk stratification, monitoring disease progression, guiding therapeutic interventions, and assessing novel anti-atherosclerotic therapies.

the plaque has subsided. By identifying areas of nascent and ongoing calcification activity, ^{18}F-NaF uptake allows us to detect regions of metabolically active plaque, thus providing complementary information to CT.[29–32] Indeed, we noted large areas of coronary CT calcium in the absence of increased ^{18}F-NaF uptake (figure 1) whereas other regions with minimal or no CT calcium had intense ^{18}F-NaF uptake (appendix) in keeping with previous observations in the aorta by Derlin and colleagues (panel).[29,32] Moreover, given that ^{18}F-NaF seems more closely aligned with the process of necrotic inflammation and plaque metabolic activity, we believe that it potentially offers major improvements to the prediction of cardiovascular risk compared with calcium scoring.

Our data have already established that ^{18}F-NaF identifies plaque with multiple high-risk features, but prospective studies are now needed in a broad range of patients to assess whether increased coronary ^{18}F-NaF activity will ultimately translate into future adverse events. If the results prove confirmatory then this technique has the potential to fundamentally alter the way we treat coronary artery disease: moving us away from the current framework based on lesion severity and ischaemia to one focused on plaque metabolism and inflammation. It could, for example, permit the identification of the vulnerable patient with single or multiple high-risk or silently ruptured plaques, providing an opportunity to treat and modify their risk to prevent future adverse cardiovascular events.

By contrast with ^{18}F-NaF, ^{18}F-FDG imaging was hampered by problems related to tracer uptake in the myocardium. Our stringent dietary recommendations resulted in suppression of myocardial activity in 70–85% of patients: a rate that compares favourably with previous studies (57–84%).[6,12,13] However, this suppression resulted in a patchy distribution of myocardial uptake that frequently obscured activity in one or more coronary vessels. Increased ^{18}F-FDG uptake might possibly occur in the culprit plaque and we failed to show this because of incomplete data or the delay in scanning. However, given its limitations, we believe that ^{18}F-FDG is unlikely to become sufficiently robust to permit its clinical application to the coronary circulation. Nevertheless, ^{18}F-FDG uptake remains an important measure of general vascular inflammation in the aorta and carotid arteries, providing complementary and distinct metabolic information to that of ^{18}F-NaF uptake.

We acknowledge that there are limitations of our study that include a lack of respiratory gating, potential partial volume artefacts, and the use of surrogate measures for coronary histology.[21] However, we believe that the totality of our comprehensive evidence using multiple approaches and imaging modalities provides a robust and cogent argument to support our contention that ^{18}F-fluoride uptake identifies vulnerable and high-risk plaques in patients with stable and unstable coronary heart disease. Further work is now needed to establish whether ^{18}F-NaF PET-CT will provide a clinically useful technique capable of improving risk stratification, monitoring disease progression, guiding therapeutic interventions, and assessing novel anti-atherosclerotic therapies.

Contributors

NVJ designed the study, undertook experiments, analysed results, and interpreted the data. ATV undertook experiments, analysed and interpreted the data, and prepared the report. MCW, ASVS, PAC, FHMC, SEY, AMF, EJRvB, and KAAF collected, analysed, and interpreted data, and prepared the report. ADF, NGU, MWHB, NLMC, and NLM collected the data and prepared the report. JHFR, MRD, and DEN contributed to the study design, supervision, and interpretation of data. DEN is the chief

investigator for the study and obtained funding for all studies. All authors participated in data interpretation. NVJ drafted the first and subsequent versions of this report with key input from MRD and DEN, and revisions from all authors, who reviewed and approved the final submitted report.

Conflicts of interest

NLM has received honoraria for Abbott Diagnostics and acted as a consultant for Abbott Diagnostics. The other authors declare that they have no conflicts of interest.

Acknowledgments

The study was funded by the Chief Scientist Office, Scotland (ETM/160) and the British Heart Foundation (PG/12/8/29371). MRD, NLM, and DEN are supported by the British Heart Foundation (CH/09/002, FS/10/024, FS/10/026). JHFR and PAC are part-funded by the NIHR Cambridge Biomedical Research Centre and the British Heart Foundation. The Wellcome Trust Clinical Research Facility and the Clinical Research Imaging Centre are supported by NHS Research Scotland (NRS) through NHS Lothian. We acknowledge the support of staff at the Edinburgh Heart Centre at the Royal Infirmary of Edinburgh, the radiography and radiochemistry staff of the Clinical Research Imaging Centre, and the histology staff at the Queens Medical Research Institute.

References

1 Naghavi M, Libby P, Falk E, et al. From vulnerable plaque to vulnerable patient: a call for new definitions and risk assessment strategies: part I. *Circulation* 2003; **108:** 1664–72.

2 Virmani R, Kolodgie FD, Burke AP, Farb A, Schwartz SM. Lessons from sudden coronary death: a comprehensive morphological classification scheme for atherosclerotic lesions. *Arterioscler Thromb Vasc Biol* 2000; **20:** 1262–75.

3 Virmani R, Burke AP, Farb A, Kolodgie FD. Pathology of the vulnerable plaque. *J Am Coll Cardiol* 2006; **47** (suppl)**:** C13–18.

4 Rogers IS, Tawakol A. Imaging of coronary inflammation with FDG-PET: feasibility and clinical hurdles. *Curr Cardiol Rep* 2011; **13:** 138–44.

5 Libby P, DiCarli M, Weissleder R. The vascular biology of atherosclerosis and imaging targets. *J Nucl Med* 2010; **51** (suppl 1)**:** 33S–37S.

6 Rogers IS, Nasir K, Figueroa AL, et al. Feasibility of FDG imaging of the coronary arteries: comparison between acute coronary syndrome and stable angina. *JACC Cardiovasc Imaging* 2010; **3:** 388–97.

7 Dweck MR, Chow MW, Joshi NV, et al. Coronary arterial 18F-sodium fluoride uptake: a novel marker of plaque biology. *J Am Coll Cardiol* 2012; **59:** 1539–48.

8 Dweck MR, Khaw HJ, Sng GK, et al. Aortic stenosis, atherosclerosis, and skeletal bone: is there a common link with calcification and inflammation? *Eur Heart J* 2013; **34:** 1567–74.

9 Dweck MR, Jones C, Joshi NV, et al. Assessment of valvular calcification and inflammation by positron emission tomography in patients with aortic stenosis. *Circulation* 2012; **125:** 76–86.

10 Tawakol A, Migrino RQ, Bashian GG, et al. In vivo 18F-fluorodeoxyglucose positron emission tomography imaging provides a noninvasive measure of carotid plaque inflammation in patients. *J Am Coll Cardiol* 2006; **48:** 1818–24.

11 Rudd JH, Warburton EA, Fryer TD, et al. Imaging atherosclerotic plaque inflammation with [18F]-fluorodeoxyglucose positron emission tomography. *Circulation* 2002; **105:** 2708–11.

12 Wykrzykowska J, Lehman S, Williams G, et al. Imaging of inflamed and vulnerable plaque in coronary arteries with 18F-FDG PET/CT in patients with suppression of myocardial uptake using a low-carbohydrate, high-fat preparation. *J Nucl Med* 2009; **50:** 563–68.

13 Cheng VY, Slomka PJ, Le Meunier L, et al. Coronary arterial ^{18}F-FDG uptake by fusion of PET and coronary CT angiography at sites of percutaneous stenting for acute myocardial infarction and stable coronary artery disease. *J Nucl Med* 2012; **53:** 575–83.

14 Thygesen K, Alpert JS, Jaffe AS, Simoons ML, Chaitman BR, White HD, and the Joint ESC/ACCF/AHA/WHF Task Force for the Universal Definition of Myocardial. Third universal definition of myocardial infarction. *Eur Heart J* 2012; **33:** 2551–67.

15 North American Symptomatic Carotid Endarterectomy Trial Collaborators. Beneficial effect of carotid endarterectomy in symptomatic patients with high-grade carotid stenosis. *N Engl J Med* 1991; **325:** 445–53.

16 Calvert PA, Obaid DR, O'Sullivan M, et al. Association between IVUS findings and adverse outcomes in patients with coronary artery disease: the VIVA (VH-IVUS in Vulnerable Atherosclerosis) Study. *JACC Cardiovasc Imaging* 2011; **4:** 894–901.

17 Murray SW, Stables RH, Hart G, Palmer ND. Defining the magnitude of measurement variability in the virtual histology analysis of acute coronary syndrome plaques. *Eur Heart J Cardiovasc Imaging* 2013; **14:** 167–74.

18 Stone GW, Maehara A, Lansky AJ, et al, and the PROSPECT Investigators. A prospective natural-history study of coronary atherosclerosis. *N Engl J Med* 2011; **364:** 226–35.

19 Ehara S, Kobayashi Y, Yoshiyama M, et al. Spotty calcification typifies the culprit plaque in patients with acute myocardial infarction: an intravascular ultrasound study. *Circulation* 2004; **110:** 3424–29.

20 Mintz GS, Nissen SE, Anderson WD, et al. American College of Cardiology clinical expert consensus document on standards for acquisition, measurement and reporting of intravascular ultrasound studies (IVUS). A report of the American College of Cardiology task force on clinical expert consensus documents. *J Am Coll Cardiol* 2001; **37:** 1478–92.

21 García-García HM, Mintz GS, Lerman A, et al. Tissue characterisation using intravascular radiofrequency data analysis: recommendations for acquisition, analysis, interpretation and reporting. *EuroIntervention* 2009; **5:** 177–89.

22 Motoyama S, Sarai M, Harigaya H, et al. Computed tomographic angiography characteristics of atherosclerotic plaques subsequently resulting in acute coronary syndrome. *J Am Coll Cardiol* 2009; **54:** 49–57.

23 Burke AP, Farb A, Malcom GT, Liang YH, Smialek J, Virmani R. Coronary risk factors and plaque morphology in men with coronary disease who died suddenly. *N Engl J Med* 1997; **336:** 1276–82.

24 Aikawa E, Nahrendorf M, Figueiredo JL, et al. Osteogenesis associates with inflammation in early-stage atherosclerosis evaluated by molecular imaging in vivo. *Circulation* 2007; **116:** 2841–50.

25 New SE, Goettsch C, Aikawa M, et al. Macrophage-derived matrix vesicles: an alternative novel mechanism for microcalcification in atherosclerotic plaques. *Circ Res* 2013; **113:** 72–77.

26 Vengrenyuk Y, Carlier S, Xanthos S, et al. A hypothesis for vulnerable plaque rupture due to stress-induced debonding around cellular microcalcifications in thin fibrous caps. *Proc Natl Acad Sci USA* 2006; **103:** 14678–83.

27 Raggi P, Callister TQ, Shaw LJ. Progression of coronary artery calcium and risk of first myocardial infarction in patients receiving cholesterol-lowering therapy. *Arterioscler Thromb Vasc Biol* 2004; **24:** 1272–77.

28 McEvoy JW, Blaha MJ, Defilippis AP, et al. Coronary artery calcium progression: an important clinical measurement? A review of published reports. *J Am Coll Cardiol* 2010; **56:** 1613–22.

29 Derlin T, Richter U, Bannas P, et al. Feasibility of 18F-sodium fluoride PET/CT for imaging of atherosclerotic plaque. *J Nucl Med* 2010; **51:** 862–65.

30 Li Y, Berenji GR, Shaba WF, Tafti B, Yevdayev E, Dadparvar S. Association of vascular fluoride uptake with vascular calcification and coronary artery disease. *Nucl Med Commun* 2012; **33:** 14–20.

31 Beheshti M, Saboury B, Mehta NN, et al. Detection and global quantification of cardiovascular molecular calcification by fluoro18-fluoride positron emission tomography/computed tomography—a novel concept. *Hell J Nucl Med* 2011; **14:** 114–20.

32 Derlin T, Tóth Z, Papp L, et al. Correlation of inflammation assessed by ^{18}F-FDG PET, active mineral deposition assessed by ^{18}F-fluoride PET, and vascular calcification in atherosclerotic plaque: a dual-tracer PET/CT study. *J Nucl Med* 2011; **52:** 1020–27.

33 Saam T, Rominger A, Wolpers S, et al. Association of inflammation of the left anterior descending coronary artery with cardiovascular risk factors, plaque burden and pericardial fat volume: a PET/CT study. *Eur J Nucl Med Mol Imaging* 2010; **37:** 1203–12.

34 Dunphy MP, Freiman A, Larson SM, Strauss HW. Association of vascular 18F-FDG uptake with vascular calcification. *J Nucl Med* 2005; **46:** 1278–84.

35 Janssen T, Bannas P, Herrmann J, et al. Association of linear (18) F-sodium fluoride accumulation in femoral arteries as a measure of diffuse calcification with cardiovascular risk factors: A PET/CT study. *J Nucl Cardiol* 2013; **20:** 569–77.